View metadata, citation and similar papers at core.ac.uk

brought to you by CORE

provided by Elsevier - Publisher Connector

Neuron, Vol. 21, 179–189, July, 1998, Copyright ©1998 by Cell Press

Reliability and State Dependence of Pyramidal Cell–Interneuron Synapses in the Hippocampus: an Ensemble Approach in the Behaving Rat

Jozsef Csicsvari, Hajime Hirase, Andras Czurko, and György Buzsáki*
Center for Molecular and Behavioral Neuroscience
Rutgers University
Newark, New Jersey 07102

Summary

Spike transmission probability between pyramidal cells and interneurons in the CA1 pyramidal layer was investigated in the behaving rat by the simultaneous recording of neuronal ensembles. Population synchrony was strongest during sharp wave (SPW) bursts. However, the increase was three times larger for pyramidal cells than for interneurons. The contribution of single pyramidal cells to the discharge of interneurons was often large (up to 0.6 probability), as assessed by the presence of significant (<3 ms) peaks in the cross-correlogram. Complex-spike bursts were more effective than single spikes. Single cell contribution was higher between SPW bursts than during SPWs or theta activity. Hence, single pyramidal cells can reliably discharge interneurons, and the probability of spike transmission is behavior dependent.

Introduction

The precise pattern of synaptic connectivity and the functionally variable strengths of the synaptic connections allow neuronal networks to perform specific computations. Most central synapses are unreliable at signaling the arrival of single presynaptic action potentials to the postsynaptic neuron, and usually multiple synaptic inputs are required to fire target cells. Recent experiments have indicated that hippocampal synapses are heterogeneous in release probability and have high failure rates (Allen and Stevens, 1994; Malinow et al., 1994). It is also recognized that central synapses are dynamic and that their modification may be the synaptic basis of memory (reviewed by Zucker, 1989; Bliss and Collingridge, 1993; Hessler et al., 1993; Zador and Dobrunz, 1997; Fisher et al., 1997; Markram et al., 1997). The signaling of principal cells to inhibitory interneurons may serve more global functions and affect the population behavior of the network (Freund and Buzsáki, 1996). These principal cell–interneuron synapses appear more reliable and display different short-term dynamics than synapses between cortical principal neurons (Gulyas et al., 1993; Arancio et al., 1994; Traub and Miles, 1995; Fortunato et al., 1996; Thomson and Deuchars, 1997; Geiger et al., 1997; Ali and Thomson, 1998; Ali et al., 1998).

Revealing the rules and mechanisms underlying the variability and reliability of synaptic communication among neurons in the intact brain is a prerequisite for understanding the behavior-dependent cooperation of neurons. However, studies in the intact brain, to date, have largely focused on the average behavior of interneurons and on their relationship to field events (Buzsáki et al., 1983; Fox et al., 1986; Ylinen et al., 1995; Skaggs et al., 1996). The present experiment addressed the following questions. First, do interneuron firing rates reflect the population behavior of pyramidal cells? Second, how reliably can a single presynaptic pyramidal cell discharge its postsynaptic interneuron? Third, do burst discharges of pyramidal cells more successfully drive interneurons than single spikes? Fourth, is the contribution of a single pyramidal cell to discharge its interneuron the same across behaviors, or does it vary with the state of the animal?

Results

Physiological Identification of Pyramidal Cells and Interneurons

The data were collected by the parallel recording of unit activity at multiple sites using wire "tetrodes" or silicon probes in the behaving rat. In the present study, only interneurons in the CA1 pyramidal layer were considered. An interneuron was classified as being in the pyramidal layer when pyramidal neurons were simultaneously recorded by the electrode. Interneurons with cell bodies in the CA1 pyramidal layer include basket cells, chandelier cells, and a portion of bistratified neurons (Sik et al., 1995; Buhl et al., 1996; Ali et al., 1998).

The two physiological criteria most frequently used to distinguish pyramidal cells and interneurons are firing frequency and spike duration (Ranck, 1973; Fox and Ranck, 1981; Buzsáki et al., 1983; Skaggs et al., 1996). In general, pyramidal cells discharge at a low rate (<5 Hz) when long epochs are considered, compared with the faster firing (>5 Hz) interneurons. Firing rate alone, however, failed to identify all interneurons (Figure 1). The spike duration of interneurons (determined at the interval between the positive peaks of the filtered trace, 0.40 ± 0.02 ms; Figure 1B) was significantly shorter than that of the pyramidal cells (0.45 ± 0.08 ms, $t[257] = 5.9$, $p < 0.0001$), but again there was some overlap between the two cell populations. An additional waveform feature, the difference between the first and second positive peaks of the filtered trace, was also calculated (Figure 1B). This spike "symmetry" parameter was empirically selected because it is sensitive to both spike duration and to the speed of action potential repolarization, a feature known to be faster in interneurons than in pyramidal cells (cf. Freund and Buzsáki, 1996). The discharge dynamics of pyramidal cells and interneurons were also characteristically different. Pyramidal cells occasionally fire complex-spike bursts of two to seven spikes at 3–10 ms interspike intervals (Ranck, 1973). This feature was reflected by their characteristic autocorrelograms, with peaks at 3–5 ms, followed by a fast exponential decay (Figure 1C). In constrast, the autocorrelograms of putative interneurons showed a slow decay. The average first moment of the autocorrelograms

*To whom correspondence should be addressed.

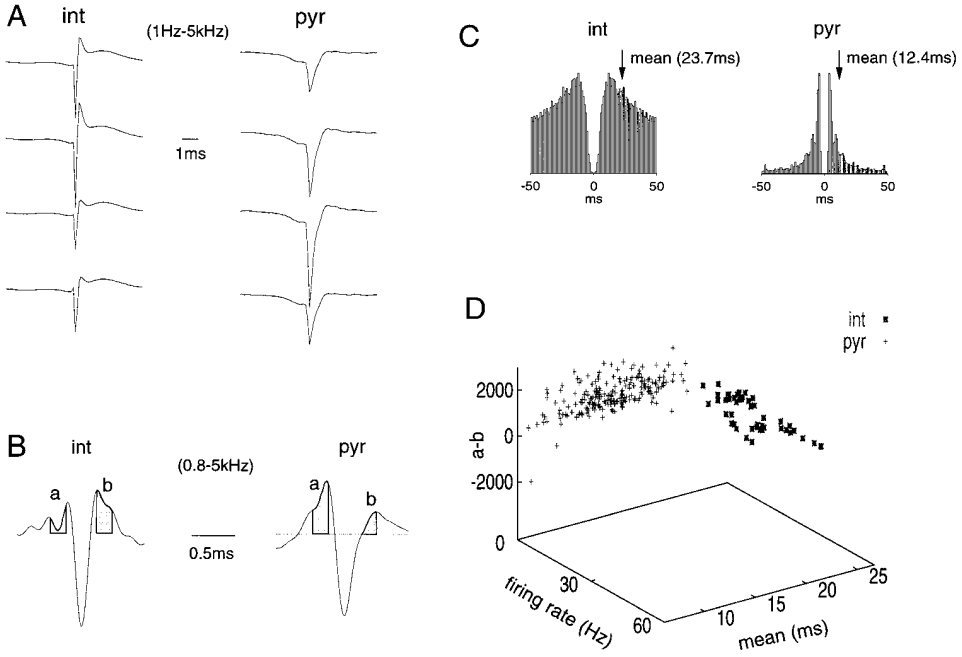

Figure 1. Physiological Identification of Interneurons

(A) Wide-band averages of the extracellular action potentials of an interneuron (int) and a CA1 pyramidal cell (pyr) recorded from the same wire tetrode. Note differences in wave shape and spike duration between the two cells.

(B) High-pass filtered derivatives of the spikes shown in (A). Shaded areas (a and b) (0.25 ms wide, ± 0.18 ms from the negative peak) reflect amplitude integral measurements used for clustering in (D).

(C) Autocorrelograms for the interneuron and the pyramidal cell. Arrows indicate the mean (first momentum) of the histograms. Note the fast decay of the histogram of the pyramidal cell.

(D) Three-dimensional plot of firing rate, spike symmetry (a and b), and the mean of the autocorrelation histograms for each neuron. Note the clear separation of the pyramidal cells from the interneuron clusters.

(i.e., the mean value) for pyramidal cells was 15 ± 0.22 ms, compared with the significantly longer values in interneurons (25 ± 0.1 ms, $t[257] = 21.7$, $p < 0.001$). The combination of the parameters (firing rate, symmetry, mean of the autocorrelograms) produced two major clusters that were putatively designated as pyramidal cells and interneurons (Figure 1D).

State-Dependent Changes of Population Synchrony in Interneurons and Principal Cells

Because interneuron and pyramidal cell populations are mutually connected, alternations in one are expected to affect the other population. These alterations include discharge pattern changes in individual cells and their population behavior. The two major population patterns of the hippocampus are (1) theta waves, associated with exploration and REM sleep, and (2) sharp waves (SPWs), which are present during consummatory behaviors and slow-wave sleep (cf. Buzsáki et al., 1983; Bland, 1986; Stewart and Fox, 1990). SPWs represent population excitation of the dendritic fields of CA1 neurons by their CA3 Schaffer collateral input. The ramp-like depolarization brought about by the CA3 pyramidal cells induces a dynamic interaction between interneurons and pyramidal cells, the result of which is a short-lived oscillatory field potential in the pyramidal layer (200 Hz "ripple"; Buzsáki et al., 1992). Coactivation of neurons within these respective physiological patterns is usually referred to as "synchronous" discharge of the neuronal population.

Since the postsynaptic effects of neuronal ensembles depend on the relative timing of the action potentials of the participating neurons ("population synchrony"), we examined the state dependence of ensemble synchrony. The percentage of simultaneously discharging neurons within a predetermined time window, relative to all recorded cells, was calculated separately for interneurons and pyramidal cells. The time window was centered to the peaks of SPWs or to the negative or positive peaks of theta waves (Figure 2A). For no-SPW epochs, consecutive, contiguous time windows were used. The calculated percentages derived from individual recording sessions were averaged. As shown in Figure 2, population synchrony dramatically increased during SPW. In a 50 ms time window, only 2% of pyramidal cells and 40%–60% of interneurons fired together during theta and no-SPW epochs. In comparison, during SPW bursts, 18% of pyramidal cells and 75% of interneurons discharged synchronously. The relative increase of ensemble synchrony from the no-SPW "baseline" to SPW was therefore much larger for pyramidal cells (5- to 9-fold) than for interneurons (2- to 3-fold). Population synchrony was highest at the peak of the SPW burst. It must be emphasized, though, that the values presented

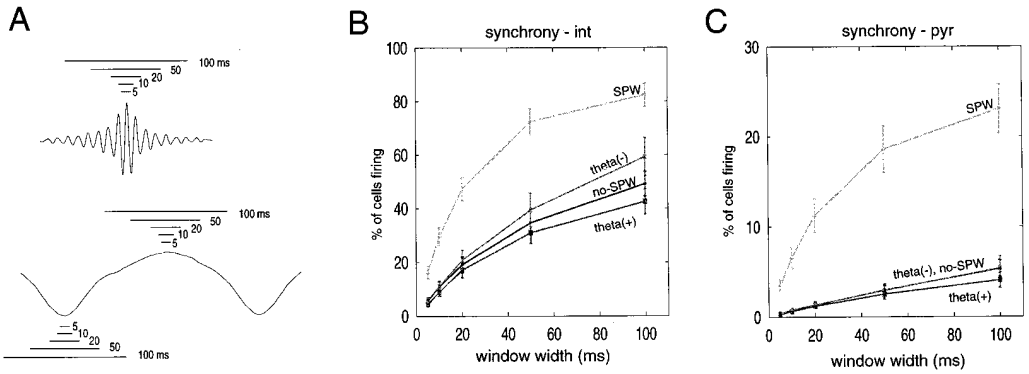

Figure 2. State Dependence of Population Synchrony

Average percent of interneurons (B) and pyramidal cells (C) firing together in time windows of different lengths (5–100 ms). Population synchrony was referenced to the peak of SPW (peak envelope of the ripple in [A]) or the positive or negative peak of theta (A). For epochs between sharp waves (no-SPW), consecutive time windows were used. Note the large increase of the population synchrony of pyramidal cells during SPW.

here for pyramidal cells are somewhat overestimated for all states because "silent" cells (Thompson and Best, 1989) were not included in the analysis.

Isolation of Monosynaptically Connected Pyramidal Cell–Interneuron Pairs

A total of 449 cross-correlograms between pyramidal cells and interneurons were examined. Some of the cross-correlation histograms showed a large, sharp peak in the 0–3 ms bins after the discharge of the reference pyramidal cell. On the basis of in vitro experiments in the hippocampus (Miles and Wong, 1986; Miles, 1990; Gulyas et al., 1993; Buhl et al., 1994; Ali et al., 1998) and neocortex (Thomson and Deuchars, 1997), short-latency peaks may reflect monosynaptic connections between the pyramidal cell and the target interneuron. Putative monosynaptic discharges of interneurons could also be revealed by superimposing successive spikes of the presynaptic pyramidal cell (Figures 3A and 3B). Inspection of superimposed traces indicated that interneuron spikes occurred after the recovery of the waveform of the presynaptic pyramidal unit. To dispel potential spurious waveform bias that may arise from the short-latency spikes, the spike features of short-latency and long-latency interneuronal spikes were clustered separately. The spike features of short-latency units and units occurring at other times were essentially identical for both interneurons (Figures 3D and 3E) and reference pyramidal cells (data not shown). This analysis therefore eliminated the possibility that artifactual waveform interactions rather than actual cellular (synaptic) interactions caused the short-latency discharges of interneurons.

Because pyramidal cells can discharge synchronously, another issue that had to be addressed is whether the putative presynaptic pyramidal cell can discharge the postsynaptic interneuron alone or only in cooperation with other pyramidal neurons. In an attempt to evaluate the contribution of a single putative presynaptic neuron, the spikes of pyramidal cells and interneurons were shuffled (see Experimental Procedures), and the shuffled correlations were subtracted from the original histograms (Figure 3C). Bin values above three standard deviations from the baseline of the derived histograms were regarded as significant ($p = 0.0013$, assuming normal distribution). Significant values were present only at the 1–3 ms bins, indicating that the shuffling procedure was powerful enough to reduce effectively the contribution of other recorded pyramidal cells (Perkel et al., 1967; Tanaka, 1983). Thirty-seven of the 449 shuffling-normalized histograms (8%) had significant peaks at monosynaptic latency (<3 ms), and these pairs were putatively classified as monosynaptically connected.

To examine further the contribution of a single neuron to the discharge of its interneuron target, we assessed the conditional probability of presynaptic synchrony from those recordings in which two or more pyramidal cells were monosynaptically connected to the same interneuron ($n = 25$ pairs). The probability that a given pyramidal cell discharged together with other connected and nonconnected pyramidal cells in a 5 ms window, preceding the interneuron spike, was 0.016 and 0.013, compared with 0.011 and 0.01 in the absence of the interneuron spike during no-SPW epochs. The conditional probability values for connected cells were larger during SPW (0.037 versus 0.032), owing to the strong population synchrony (Figure 2). None of these comparisons was statistically significant. These calculations indicate that although a single pyramidal cell may discharge a postsynaptic interneuron, the contribution of other unrecorded pyramidal neurons cannot be ruled out in all behavioral states. For the estimation of monosynaptic "contribution," previous studies used the ratio between the peak bin values at monosynaptic latency and the average of the remaining bin values of the histograms (Tanaka, 1983; Reid and Alonso, 1995). Since in our study, the firing rate varied as a function of the theta, SPW, and no-SPW states, the variability of the "background" bins also varied. To normalize for this variability, the peak bin values at monosynaptic latency were divided by the standard deviation of the bin values.

Pyramidal Cell–Interneuron Pairs: Single Spikes Versus Complex-Spike Bursts

For pairs with significant peaks at monosynaptic latency ($n = 37$), the average probability of spike transmission

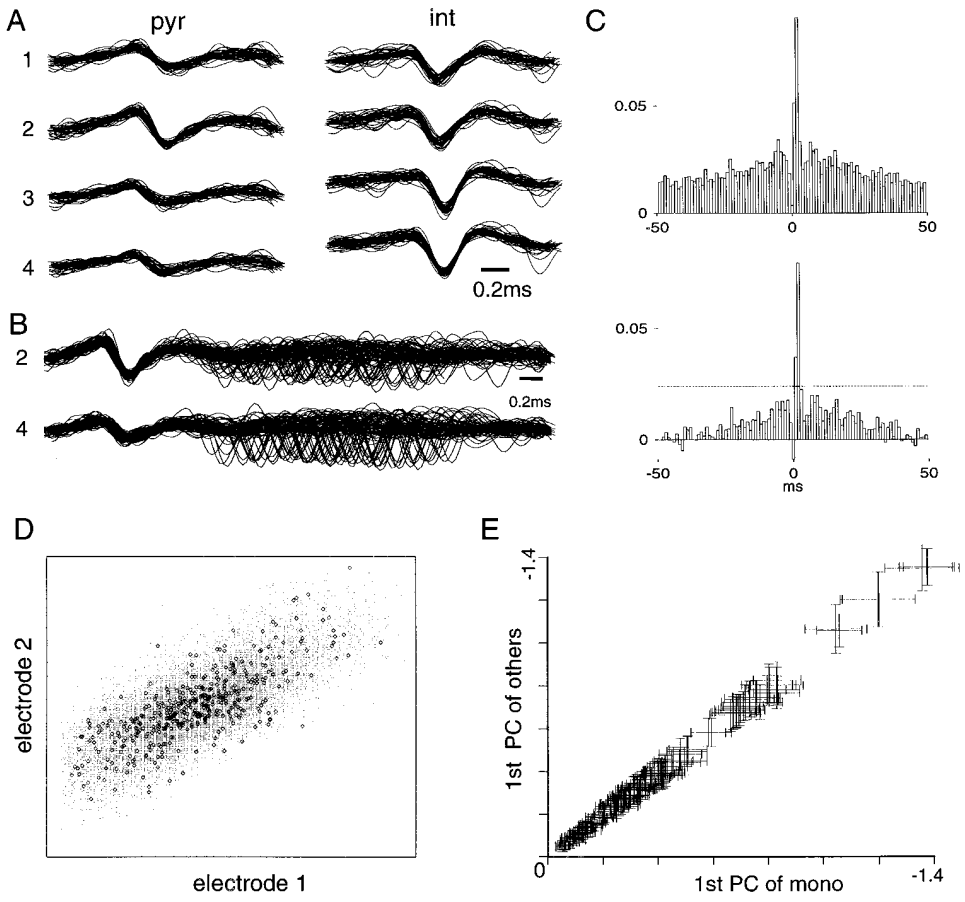

Figure 3. Monosynaptic Drive of an Interneuron by a Pyramidal Cell

(A) Superimposed waveforms of a pyramidal cell (pyr) and an interneuron (int) recorded by a wire tetrode.

(B) Expanded superimposed events from recording sites two and four. Note short latency (<2 ms) occurrence of the interneuron discharge after the pyramidal cell spike.

(C) Cross-correlogram of the two cells. Reference event, action potential of the pyramidal cell (n = 2,646 spikes). Note large, sharp peak in the 0–1 and 1–2 ms bins (total of 22,762 interneuron spikes). To remove the contribution of neurons, the spikes of the pyramidal cell and the interneuron were shuffled, and the shuffled values were subtracted (bottom histogram). Dotted lines indicate 3 SD of the mean ($p < 0.002$).

(D) Spike features of short-latency (diamonds) and all other interneuron spikes (dots). Same neuron as in (A–C).

(E) Spike features (1st PCs) of short-latency (1st PC of mono) versus all other spikes (1st PC of others) for all interneurons (mean ± SD). Four data points, corresponding to the four recordings sites, are shown for each cell. The linear relationship (X = Y) indicates that short-latency spikes had the same wave forms as all other spikes of the same neuron.

from a putative presynaptic pyramidal cell to a postsynaptic interneuron was 12% ± 2.2%, with an average latency of 1.56 ± 0.03 ms (range, 0.9–1.95 ms). Because pyramidal cells can emit either a single spike or a complex-spike burst, we examined whether complex-spike patterns were more effective in driving target interneurons than single spikes. Repetitive spike discharges within 7 ms were regarded as part of the complex-spike burst. The average number of spikes per complex-spike burst was 2.25 ± 0.02. Single spikes and the first action potential of the complex-spike burst were followed by an interneuron spike with a similar probability (Figure 4D). Subsequent spikes of the bursts were also effective. In some pairs, each of the three to five action potentials of complex-spike bursts was followed by an interneuron spike (Figures 4A–4C). For all pairs, the probability of the interneuron discharge was significantly higher after a complex-spike burst, regarded as a single event, than after a single spike (Figure 4D; 0.22 versus 0.12, $F = 3.44$, $p < 0.02$). The effectiveness of the second spike depended on whether the first spike was correlated with an interneuron action potential. When the first spike failed to discharge the interneuron (zero probability), the second spike could still be followed by an interneuron spike (Figure 4D, "1st fail"). On the other hand, when the first spike was successful (1.0 probability), the second spike of the complex-spike burst was less likely to be followed by an interneuron spike (Figure 4D, "1st fire").

Pyramidal Cell–Interneuron Pairs: State-Dependent Transmission

Comparison of the pyramidal cell–interneuron cross-correlograms, created from spikes collected during theta, no-SPW, and SPW epochs, suggested that the efficacy of synaptic transmission depended on the state of the network. Figure 5 illustrates a case when two pyramidal

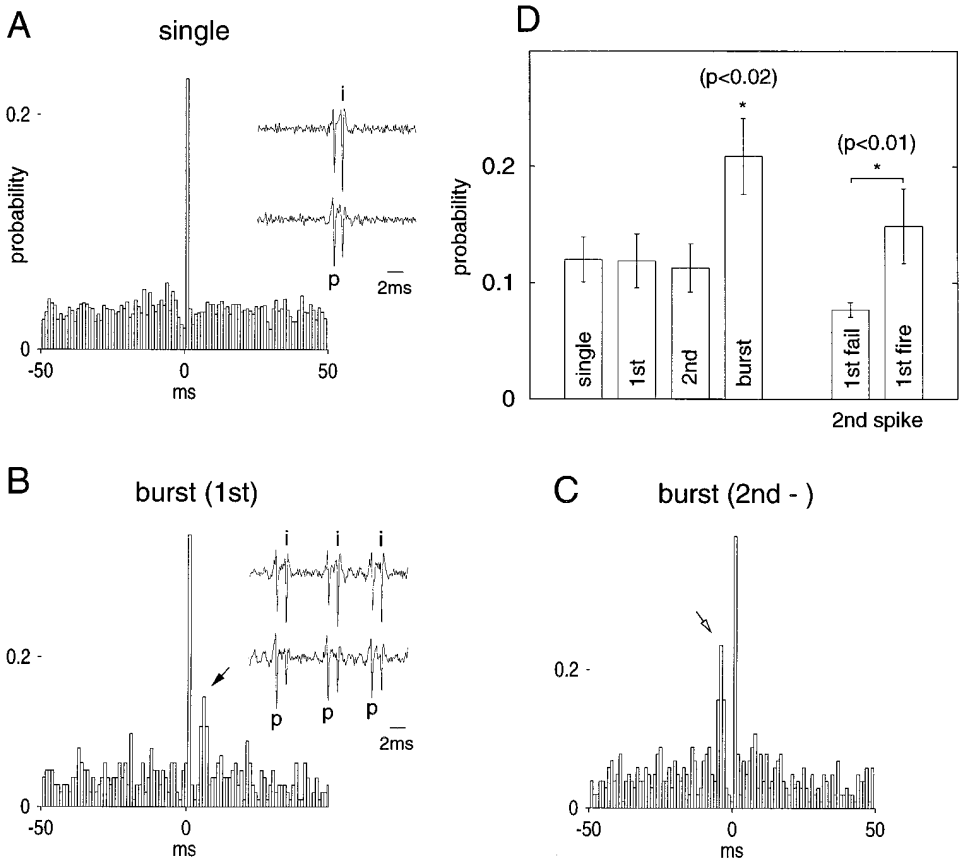

Figure 4. Complex-Spike Bursts Contribute More Effectively to Interneuron Spikes Than Single Spikes

Cross-correlograms between a pyramidal cell and an interneuron pair.

(A) Reference event, single spikes of the pyramidal cell.

(B) Reference event, first spike of complex-spike bursts. Note a secondary peak (arrow).

(C) Reference event, second (2nd) to nth spike of complex-spike bursts. Arrow indicates spike bins that correlate with the previous spikes of the complex-spike burst.

(A, inset) Traces from two electrodes showing a single pyramidal cell spike (p) and an interneuron spike (i).

(B, inset) Complex-spike burst (p) and triplet discharge in the interneuron (i). Histograms are based on at least 1,300 spikes for pyramidal cells and 83,000 spikes for the interneuron.

(D) Pooled data for 34 pairs. Probability of interneuron discharge following a single spike (single), the first and second spikes (1st, 2nd), and all spikes (burst) of complex-spike bursts. Right columns show the probability of an interneuron spike following the second spike of a complex-spike burst when the first spike of the burst either was not (1st fail) or was (1st fire) followed by an interneuron discharge.

cells innervated a common interneuron. Both pyramidal cells discharged the target interneuron with a high overall probability, although one of the two (P1) was consistently more successful than the other (P2). In this animal, spike transmission probability was highest during theta activity (wheel running) for both pairs. During SPW bursts, one of the presynaptic pyramidal cells (P1) contributed little to the discharge of the interneuron, whereas the other pyramidal cell (P1) continued to be effective, albeit at a lower probability than during theta. When all pairs in all rats were averaged, the highest probability values were obtained during no-SPW epochs and were lowest during SPW bursts ($F = 9.02$, $p < 0.001$, ANOVA).

Spatial Topography and Efficacy of Pyramidal Cell–Interneuron Connections

The number of putative monosynaptic connections between pyramidal cells and interneurons is underestimated here because the spike transmission probability method, as opposed to recording excitatory postsynaptic potentials (EPSPs), may not reveal anatomically connected pairs that have very high transmission failures. Overall, 8% of all pairs examined had putative monosynaptic connections. This value is somewhat smaller than estimated by paired recordings from identified pyramidal cells (13%; Ali et al., 1998). The connection probability was largely a function of the distance between the presynaptic pyramidal cell and the postsynaptic interneuron. Of the 194 pyramidal–interneuron pairs recorded by the same electrode, 34 (17.6%) had significant peaks at monosynaptic latency. In contrast, only 3 of the 256 pyramidal–interneuron pairs (1.17%), recorded with two separate electrodes at >300 μm from each other, had functional connections. The contribution, as estimated by the probability of spike transmission, varied from 0.036–0.6 in different pairs (all correlations were significant at $p < 0.002$). This 16-fold range is comparable to the variability of unitary EPSPs across different

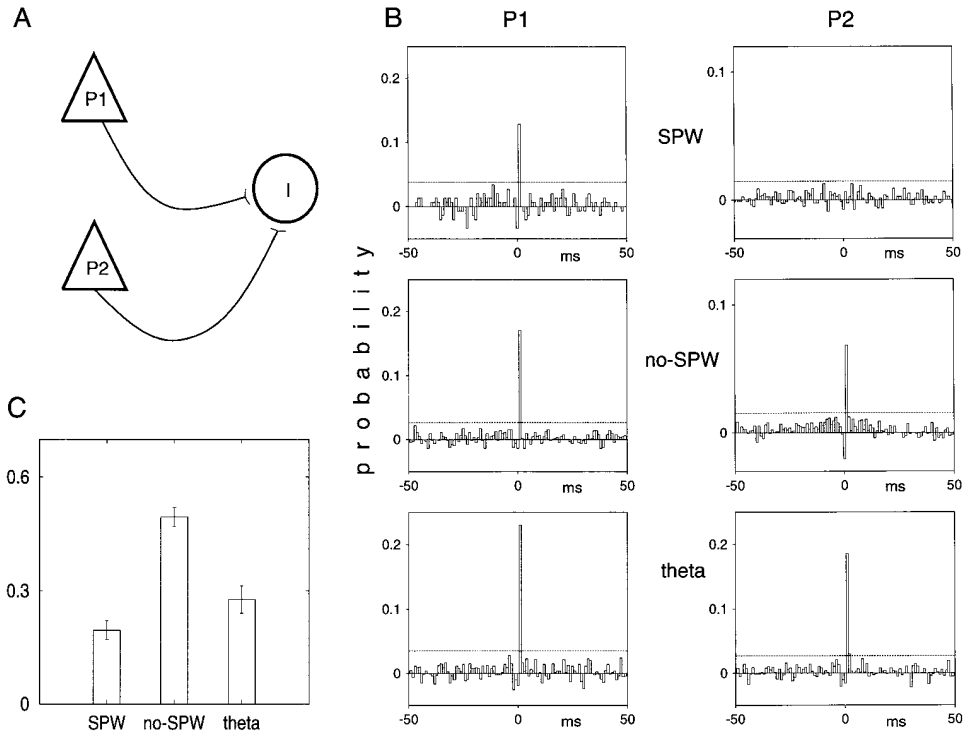

Figure 5. State Dependence of Single Pyramidal Cell Contribution to Interneuron Spike

(A) Two simultaneously recorded pyramidal cells (P1, P2) converge onto an interneuron (I).

(B) Shuffling-corrected cross-correlograms between P1, P2, and the interneuron during different population states. Note the absence of a monosynaptic peak during SPW for neuron P2 and of reliable monosynaptic peaks during theta and no-SPW epochs. Dotted lines, 3 SD from baseline ($p < 0.002$).

(C) Pooled data for all pairs ($n = 37$). For the estimation of single cell contribution (Tanaka, 1983), the values of the short-latency bins (<2 ms) were divided by SD. Ordinate, relative probabilities in the three different states.

pyramidal–interneuron pairs in the slice (Ali et al., 1998). Part of this variability could be attributed to the slightly different behavioral states across sessions and among animals, as shown above. However, the contribution of a single pyramidal cell to the discharge of the target interneuron also varied within the same animal when several putative presynaptic pyramidal neurons were recorded simultaneously with an interneuron (Figures 5 and 6). Since the highest spike transmission probabilities were obtained from pairs where the spike amplitude of both interneuron and pyramidal cells was large, we hypothesized that the distance between the neurons may affect synaptic efficacy. The rationale of this approach is that the amplitude of the extracellular spike is a function of the distance between the recording electrode and the cell body. Recording from larger amplitude interneurons increases the probability that adjacent presynaptic pyramidal cells are also recorded by the same electrode. A multivariate regression analysis revealed a significant correlation between the amplitude of the recorded extracellular spikes and the spike-to-spike latency ($F = 13.6$, $r = -0.68$, $p < 0.001$), as well as spike transmission probability ($F = 12.5$, $r = 0.67$, $p < 0.001$). The relationship between pyramidal cell–interneuron spike latency and spike transmission probability is shown in Figure 6D. These measurements suggest that the contribution of the pyramidal cell in discharging the postsynaptic interneuron decreased exponentially as a function of discharge delay. Overall, these observations suggest that at least part of the variability of the synaptic strength between pyramidal cells and interneurons can be explained by their topographic relationship.

Discussion

The major findings of the present experiments are that (1) population synchrony between pyramidal cells and interneurons varies as a function of behavior, (2) burst discharges of pyramidal cells are more effective in driving interneurons than single spikes, and (3) the excitatory transmission from pyramidal cell to interneuron shows high variability; interneurons in the vicinity of pyramidal cells are driven more effectively than distal ones. The observations also suggest that the contribution of a single pyramidal cell to the discharge of its target interneuron varies with the state of the hippocampal network.

Interactions Between CA1 Pyramidal Cells and Interneurons

All interneurons included in the present study were recorded from the pyramidal layer. Interneuron classes with cell bodies in this layer include mostly basket and chandelier cells and a portion of bistratified cells (Sik et al., 1995; Buhl et al., 1996; Ali et al., 1998). Basket and

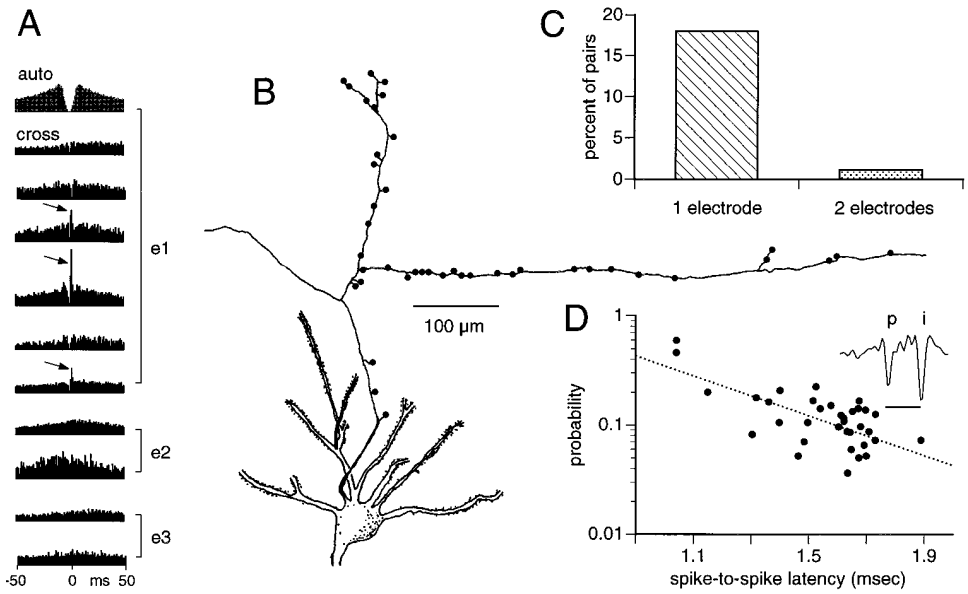

Figure 6. Local Control of Interneuron Discharge

(A) Autocorrelogram of an interneuron (gray) and cross-correlation histograms of the interneuron with simultaneously recorded pyramidal cells from the same electrode (e1) and adjacent electrodes (e2, e3). Note sharp peaks at monosynaptic latency (arrows) in three of the six pyramidal cells recorded with the same tetrode.

(B) Distribution of axon collaterals and boutons (black circles) of an in vivo filled CA1 pyramidal cell (E. C. Papp and G. B., unpublished data). Note higher density of boutons in the vicinity of the cell body. Dendrites are truncated.

(C) Percent of pyramidal–interneuron cell pairs with significant peaks at monosynaptic latency (<3 ms) from all experiments. One (1) electrode, neuron pairs recorded with the same electrode; two (2) electrodes, neuron pairs recorded with adjacent electrodes.

(D) Relationship between discharge latency (p, pyramidal cell; i, interneuron) and discharge probability. Each dot represents a pyramidal cell–interneuron pair with a significant ($p < 0.002$) peak at monosynaptic latency. Linear regression, -0.73 ($F = 36.1$, $p < 0.0001$). Inset calibration, 1 ms.

chandelier cells are believed to be critical in the maintenance of network oscillations and in the timing of pyramidal action potentials (cf. Buzsáki and Chrobak, 1995; Jefferys et al., 1996).

Excitatory afferents to basket and chandelier cells are similar to inputs to CA1 pyramidal cells. Since these interneurons are reciprocally connected to pyramidal cells (Buhl et al., 1994), they are excited by both CA3 and CA1 pyramidal cells during SPWs. Nevertheless, population synchrony was 3- to 4-fold larger for the pyramidal cells during SPWs than that of the interneurons (cf. Figures 2B and 2C). These findings indicate that the activity of basket and chandelier cells does not simply reflect the average discharge rates of pyramidal cells and that the functional connectivity of these cells changes dynamically.

Reliability of Synaptic Transmission Between Pyramidal Cells and Interneurons

Some important findings of the present experiment were the high proportion of functionally coupled neurons and the high reliability of spike transmission in some pyramidal cell–interneuron pairs. High spike transmission probability was observed only when neuron pairs were recorded with the same electrode. Since extracellular unit activity from the same neurons cannot be recorded by two electrodes with >100 μm horizontal separation in the pyramidal layer (Nadasdy et al., 1998), the recorded pairs were likely located within a 100 μm diameter cylinder. This volume contains ~500 pyramidal cells (Aika et al., 1994). Because in this volume 17.8% of the simultaneously recorded pyramidal cell–interneuron pairs were functionally connected, we estimate that ~100 pyramidal cells may converge on a pyramidal layer interneuron.

The success or failure of a presynaptic neuron to discharge its postsynaptic partner depends on various factors, including its synchrony with other neurons, the pattern of presynaptic neuronal discharge, axonal conductance failures, presynaptic control of transmitter release, the number of release sites, the number of quanta released, sensitivity of the postsynaptic receptors, the polarization level of the membrane, and the immediate history of the postsynaptic cell (Allen and Stevens, 1994; Lisman, 1997; Thomson and Deuchars, 1997; Tsodyks and Markram, 1997; Abbott et al., 1997). Previous experiments in vitro have indicated that synapses among principal cells are heterogeneous in release probability and are characterized by frequent transmission failures (Miles and Wong, 1986; Otmakhov et al., 1993; Allen and Stevens, 1994; Raastad, 1995; Bolshakov and Siegelbaum, 1995; Dobrunz and Stevens, 1997; Thomson and Deuchars, 1997; Abbott et al., 1997; Markram et al., 1997). Excitatory transmission between principal cells and interneurons, however, appears more reliable. In paired recordings from CA1 pyramidal cells and interneurons, including identified basket, chandelier, bistratified, and O-LM neurons, pyramidal cells evoked EPSPs in interneurons with high probability, although spike discharges were only rarely observed (Lacaille et al., 1987; Buhl et al., 1994, 1996; Ali and Thomson, 1998;

Ali et al., 1998). The probability of EPSP transmission between CA3 pyramidal cells and pyramidal layer interneurons was similarly high (Gulyas et al., 1993; Fortunato et al., 1996), and in a single study, up to 0.6 spike transmission probability was observed (Miles, 1990).

The similarity of these previous in vitro observations and the present data suggest that monosynaptic peaks in the cross-correlograms reflect that interneurons could be discharged by a single presynaptic pyramidal neuron. Although near-simultaneous discharge of pyramidal cells cannot be ruled out with certainty, several observations indicate that the contribution of a single cell could be large. First, spurious, short-latency drive by a common input (Perkel et al., 1967), e.g., by the associational, commissural, or entorhinal afferents, is unlikely because stimulation of these pathways activates interneurons prior to the pyramidal cells (Fox and Ranck, 1981; Buzsáki et al., 1983), i.e., opposite to the observed correlations. Second, the fast time course of the EPSPs in interneurons (2–10 ms half-time; Miles, 1990; Geiger et al., 1997; Ali et al., 1998) reduces the opportunity for spatiotemporal summation, compared with pyramidal cells. Although synchronous discharge of pyramidal cells was present during SPW in such a short time window, the contribution of a single cell to the interneuron spike was, in fact, larger during theta and no-SPW epochs when $<0.26\%$ of pyramidal cells discharged together in a 5 ms window (Figure 2). Third, complex-spike bursts of a pyramidal cell were followed by an interneuron spike twice as often as by single spikes. Although our methods cannot unequivocally refute the contribution of unrecorded pyramidal cells, the findings are compatible with the suggestion that single pyramidal cells may effectively discharge interneurons (Miles, 1990; Traub and Miles, 1995).

The contribution of a single cell varied $>$10-fold among the different pairs. The size of single spike–evoked unitary EPSPs in interneurons also varies extensively, even when the postsynaptic cells belong to the same interneuron class (Gulyas et al., 1993; Buhl et al., 1996; Ali and Thomson, 1998; Ali et al, 1998). The source of this large variability is not clear. Use-dependent potentiation of AMPA synapses on interneurons is also controversial (McBain and Maccaferri, 1997). The present observations suggest that interneurons in the immediate vicinity of the presynaptic pyramidal cell are discharged more effectively than interneurons located more distally. First, high spike transmission probability was observed only when the neurons were recorded with the same electrode. Second, a reliable inverse correlation was found between spike transmission time and single cell contribution. This relationship may be accounted for by assuming that adjacent interneurons are innervated by more synapses than distal ones. The higher density of axon collaterals and synaptic boutons of the pyramidal cells in the vicinity of the soma (E. C. Papp and G. B., unpublished data) is compatible with such a structural explanation. However, previous studies suggest that pyramidal cells innervate their target interneurons by a single release site (Gulyas et al., 1993; Buhl et al., 1996). An alternative morphological explanation is that pyramidal cells innervate progressively more distal dendritic sites with distance. Indeed, the location of synaptic contacts is believed to be an important factor in shaping the EPSP time course (Rall, 1967). A physiological alternative to these anatomical explanations is that axon conductance failures are more frequent in distal axon branches than in axon collaterals close to the soma; therefore, nearby interneurons are discharged more reliably. Independent of the reasons, our findings demonstrate that spike transmission between pyramidal cells and interneurons in the CA1 pyramidal layer can be very efficient. The observed high reliability of pyramidal–interneuron spike transmission may explain why activity of certain interneurons in the behaving rat can also display some "spatial selectivity," a characteristic feature of hippocampal pyramidal cells (McNaughton et al., 1983; Kubie et al., 1990).

Spike Transmission Between Pyramidal Cells and Interneurons Is State Dependent

Observations at the population level indicated that net inhibition and excitation varied as a function of behavior. Although some interneurons transiently increased their discharge rates up to 200 Hz during SPW, the population synchrony of pyramidal cells exceeded that of the interneurons. At least part of this disproportional change may be explained by the decreased spike transmission between pyramidal cells and interneurons. The contribution of single pyramidal cells to the discharge of target interneurons was least effective during the SPW state. The diminished drive of interneurons during SPW may be explained by various simultaneously acting factors. Successful discharge of the interneuron by a single pyramidal neuron will make the interneuron refractory to other pyramidal cells, at least for the duration of the spike. Inhibitory connectivity among the interneuronal populations may also account for the nonlinear relationship between increasing population synchrony of interneurons and pyramidal cells (Tsodyks et al., 1997). Selective presynaptic suppression of glutamate release on interneurons (Shigemoto et al., 1996) is yet another mechanism to decrease the efficacy of pyramidal cells in driving interneurons during SPW. Independent of the mechanisms, our findings demonstrate that the strength of synaptic connectivity between pyramidal cells and interneurons is variable and state dependent. The dynamically variable strengths of the individual pyramidal–interneuron connections, in turn, may contribute significantly to changing population synchrony among principal cells and may allow them to perform specific computations.

Monosynaptic Efficacy and Population Oscillation

By way of their synchronous oscillatory behavior, interneurons can time the occurrence of action potentials of principal cell populations. In many forms of network oscillations, interneurons appear to be the cause of the rhythm (cf. Buzsáki and Chrobak, 1995). Nevertheless, the phase relationship of active pyramidal cells can deviate from the the background population average. For example, sequentially occurring spikes of pyramidal cells gradually shift to earlier phases of the theta cycle as the rat approaches and passes through the cell's place field (O'Keefe and Recce, 1993). A potential consequence of the high efficacy of the pyramidal–interneuron

synapse, as demonstrated here, is that the action potentials of the target interneuron would show phase precession similar to its presynaptic place cell(s). The hypothesized result is a local, phase-shifted discharge in the interneuron innervated subnet. Testing this hypothesis will require simultaneous recordings from the members of these functional subnets.

Experimental Procedures

Surgery

Nine male rats of the Sprague-Dawley strain (400–900 g) were used. They were anesthetized with a mixture (4 ml/kg) of ketamine (25 mg/ml), xylazine (1.3 mg/ml), and acepromazine (0.25 mg/ml) and placed in the stereotaxic apparatus. Pairs of stainless steel wires (60 μm in diameter) with a 0.5 mm vertical tip separation were placed into the fimbria-fornix/hippocampal commissure (AP = −0.8, L = 0.5, V = −4.2) to stimulate the commissural afferents to the CA1 region. Both wire electrodes (seven rats) and silicon electrode arrays (two animals) were used for the recording of neuronal activity. Wire tetrodes (Recce and O'Keefe, 1989, Soc. Neurosci., abstract) consisted of four 13 μm enamel-coated nichrome wires (H. P. Reid Company, Palm Coast, FL) bound together by twisting them and then melting their insulation (Gray et al. 1995). The tips were gold plated to reduce electrode impedances to 400–600 kΩ. The wire tetrodes were attached to a multidrive array, and four to twelve electrodes were independently moved during the experiment. Silicon electrode arrays were fabricated using the technology of integrated circuits. The shanks of the silicon probes were separated by either 150 or 300 μm. Each shank contained four recording sites (9 × 12 μm platinum pads) with 25 μm vertical spacings (Ylinen et al., 1995). The platinum recording sites were oxidized before the surgery to reduce tip impedances to 400–600 kΩ.

During surgery, a hole was drilled above the dorsal hippocampus (centered at −4.0 mm posterior to bregma and 3.0 mm lateral from the midline). After cutting the dura mater, the electrode assembly was positioned into the surface layers of the neocortex. The brain was sealed by a mixture of paraffin and mineral oil. The microdrive was then fixed to the skull with dental cement. Six to twelve supporting screws (0.8 mm) were also mounted in the skull. Two 50 μm single tungsten wires (with 2 mm of the insulation removed) were inserted into the cerebellum and served as ground and reference electrodes. The microdrive and the head connector were protected by a copper mesh wall that also served as electrical shielding.

Recording and Data Processing

Several days after the surgery, the electrodes were slowly (100–300 μm movement per day) moved into the hippocampus. Instrumentation amplifier dyes built in the female connector (BAK Electronics, Germantown, MD) were used to reduce cable movement artifacts. Positioning of the recording electrode in the hippocampus was aided by the commissurally evoked responses (Ylinen et al., 1995). Electrical activity was recorded during sleep while the rat was in its home cage (session 1) followed by exploration in the home cage (session 2). Three rats were trained to run in a wheel for a water reward (Buzsáki et al., 1983). For these animals, session 2 contained running and drinking behaviors. The electrodes were moved daily and new sets of cells were recorded. After amplification (5,000×–10,000×) and band-pass filtering (1 Hz–5 kHz, Model 12–64 channels; Grass Instruments, Quincy, MA), field potentials and extracellular action potentials were recorded continuously, using parallel-connected PC486 computers with ISC-16 analog-to-digital converter boards (12-bit resolution; RC Electronics, Santa Barbara, CA) or a 32-channel DATAMAX system (16-bit resolution; RC Electronics). The recorded data were digitized at 10 or 20 kHz. Recording sessions lasted from 15 min to 50 min. After each recording session, the data were transferred to a 133 MHz Pentium personal computer running under a LINUX operating system and stored on 4 mm DAT tapes. The data were analyzed offline. Analysis programs were written in C programming language and run under a UNIX (LINUX) operating system in an XWindow environment. For statistical analyses, a STAT 5.4 UNIX software package (Perlman, 1980) and a SYSTAT 5.4 were used.

Spike Sorting

The continuously recorded wide-band signals were digitally high-pass filtered (0.8–5 kHz). The power (root mean square) of the filtered signal was computed in a sliding window (0.2 ms) for spike detection (Bankman et al., 1993). Standard deviation was calculated to estimate the variance of the baseline noise and to establish a detection threshold. Spikes with power of >5 times the standard deviation from the baseline mean were extracted. The extracted spike waveforms were separated on the basis of their spike amplitude and wave shape. The spike waveforms were reconstructed to 40 kHz by using the principles of the sampling theorem (Press et al., 1992), and the peaks of the original and reconstructed waveforms were realigned. Instead of simple peak-to-peak measurement of the spike amplitude, all sampled amplitude values ± 0.5 ms from the peak were used in order to reduce noise-induced variance. The information encoded in the amplitude values was compressed using principal component analysis (PCA). The PCA method has been successfully used before to discriminate units in single electrode recordings (Abeles and Goldstein, 1977), and these principles were used here for multisite recordings. Typically, the first three principal components (PCs) were calculated for each channel. Therefore, a single spike was represented by twelve waveform parameters as a twelve-dimensional feature vector. Units were identified and isolated by a graphical clustering method referred to as cluster cutting (Wilson and McNaughton, 1993; Skaggs et al., 1996). This technique exploits the observation that single units tend to form dense patches of points (clusters) when waveform parameters derived from different recording sites are displayed. A custom-made XWindow software (gclust) was used to plot selected pairs of waveform parameters and to select clusters by drawing a polygon around cluster borders. The program calculated the autocorrelograms of clusters to verify whether a chosen cluster represented the activity of a single cell. If no clear refractory period (<3 ms) was detected in the autocorrelogram, additional feature combinations were examined to further subdivide the cluster until a clear refractory period was present. Only units with clear refractory periods are included in the present analysis. In addition, cross-correlation histograms of all possible pairs recorded from a given tetrode or silicon probe were calculated and examined for a symmetrical gap in the center bins. The gaps (common refractoriness) indicated that the initial clusters represented activity of the same unit (Fee et al., 1996), and therefore those clusters were merged. These combined methods produced four to six (occasionally up to nine) well-isolated neuron clusters per electrode shank. Neurons recorded simultaneously from four to twelve sites in the CA1 pyramidal layer were analyzed this way. Neurons with very low firing rates (silent cells; Thompson and Best, 1989) could not be reliably tested with these methods and were deleted from the database.

Cross-Correlation Analysis

Because the number of action potentials used for the construction of autocorrelograms and cross-correlograms varied from cell to cell, the histograms were normalized by dividing each bin by the number of reference events. A second, shuffled cross-correlation histogram was also calculated by shifting the spike train of the second cell with a fixed (100 ms) time interval. This procedure retained the internal dynamics of spiking for both trains but eliminated a causal relationship between them. The shuffled histogram was subtracted from the original in order to reduce the effect of random interactions. Because population synchrony increases during SPW bursts, the incidence of spurious correlations can also increase. This effect is similar to stimulus-dependent correlations (Perkel et al., 1967). To eliminate the synchronizing effect of SPW bursts, shuffled histograms were calculated during SPWs by cross-correlating the action potential of the reference cell in SPW_i with the spike of the second cell in SPW_{i+1}. Normal distribution was assumed for the estimation of the significance of correlation peaks (Abeles, 1982; Reid and Alonso, 1995). The significance level was set at three standard deviations from the mean ($p = 0.0013$).

Detection of SPWs, Ripples, and Theta Patterns

First, the wide-band recorded data was digitally band-pass filtered (150–250 Hz). The power (root mean square) of the filtered signal was calculated for each electrode and summed across electrodes. During SPW ripple episodes, the power substantially increased, enabling us to determine the beginning, peak, and end of individual ripple episodes. The threshold for ripple detection was set to seven standard deviations above the background mean. Theta epochs in the wheel running task, exploration, and REM sleep were detected by calculating the ratio of the theta (5–10 Hz) and delta (2–4 Hz) frequency bands in 2.0 s windows. A Hamming window was used during the power spectra calculations. The theta–delta power ratio automatically marked periods of theta activity. The exact beginning and end of theta epochs were manually adjusted. Next, the individual theta waves were identified. The wide-band signal was digitally filtered in the 5–28 Hz range. This relatively wide band was chosen empirically to avoid phase delays in peak detection. The negative peaks of the theta waves were detected because positive peaks were less prominent. The intervals between successive negative peaks served as reference time points for normalizing theta cycle lengths.

Histological Procedures

Following completion of the experiments, the rats were deeply anesthetized and perfused through the heart first with cacodylate buffered saline (pH 7.5), followed by a cacodylate buffered fixative containing 4% paraformaldehyde and 5.9% calcium chloride (pH 7.5). Brains were left in situ for 24 hr, removed, and then postfixed in the same solution for 1 week. The brains were sectioned by a Vibratome at 100 μm in the coronal plane. The sections were stained with the Gallyas silver method (Gallyas et al., 1990). After staining, they were dehydrated, mounted on slides, and coverslipped.

Acknowledgments

We thank C. King, R. Miles, M. Recce, and the anonymous reviewers for their constructive comments on the manuscript. This work was supported by the National Institutes of Health (NS34994, MH54671, 1P41RR09754), the Human Frontier Science Program, and the Whitehall Foundation.

Received January 1, 1998; revised May 6, 1998.

References

Abbott, L.F., Varela, J.A., Sen, K., and Nelson, S.B. (1997). Synaptic depression and cortical gain control. Science *275*, 220–224.

Abeles, M. (1982). Quantification, smoothing, and confidence limits for single-units' histograms. J. Neurosci. Methods *5*, 317–325.

Abeles, M., and Goldstein, M.H. (1977). Multispike train analysis. Proc. IEEE *65*, 762–773.

Aika, Y., Ren, J.Q., Kosaka, K., and Kosaka, T. (1994). Quantitative analysis of GABA-like-immunoreactive and parvalbumin-containing neurons in the CA1 region of the rat hippocampus using a stereological method, the disector. Exp. Brain Res. *99*, 267–276.

Ali, A.B., and Thomson, A. (1998). Facilitating pyramidal to horizontal-alveus interneurone inputs: dual intracellular recordings in slices of rat hippocampus. J. Physiol. *507*, 185–199.

Ali, A.B., Deuchars, J., Pawelzi, H., and Thomson, A. (1998). CA1 pyramidal to basket and bistratified EPSPs: dual intracellular recordings in rat hippocampal slices. J. Physiol. *507*, 201–217.

Allen, C., and Stevens, C.F. (1994). An evaluation of causes for unreliability of synaptic transmission. Proc. Natl. Acad. Sci. USA *91*, 10380–10383.

Arancio, O., Korn, H., Gulyas, A., Freund, T., and Miles, R. (1994). Excitatory synaptic connections onto rat hippocampal inhibitory cells may involve a single transmitter release site. J. Physiol. *481*, 395–405.

Bankman, I.N., Johnson, K.O., and Schneide, W. (1993). Optimal detection, classification, and superposition resolution in neural waveform recordings. IEEE Trends Biomed. Eng. *40*, 836–841.

Bland, B.H. (1986). The physiology and pharmacology of hippocampal formation theta rhythms. Prog. Neurobiol. *26*, 1–54.

Bliss, T.V., and Collingridge, G.L. (1993). A synaptic model of memory: long-term potentiation in the hippocampus. Nature *361*, 31–39.

Bolshakov, V.Y., and Siegelbaum, S.A. (1995). Regulation of hippocampal transmitter release during development and long-term potentiation. Science *269*, 1730–1734.

Buhl, E.H., Halasy, K., and Somogyi, P. (1994). Diverse sources of hippocampal unitary inhibitory postsynaptic potentials and the number of synaptic release sites. Nature *368*, 823–828.

Buhl, E.H., Szilagyi, T., Halasy, K., and Somogyi, P. (1996). Physiological properties of anatomically identified basket and bistratified cells in the CA1 area of the rat hippocampus *in vitro*. Hippocampus *6*, 294–305.

Buzsáki, G., and Chrobak, J.J. (1995). Temporal structure in spatially organized neuronal ensembles: a role for interneuronal networks. Curr. Opin. Neurobiol. *5*, 504–510.

Buzsáki, G., Leung, L.W., and Vanderwolf, C.H. (1983). Cellular bases of hippocampal EEG in the behaving rat. Brain Res. *287*, 139–171.

Buzsáki, G., Horvath, Z., Urioste, R., Hetke, J., Wise, K. (1992). High-frequency network oscillation in the hippocampus. Science *256*, 1025-1027.

Dobrunz, L.E., and Stevens, C.F. (1997). Heterogeneity of release probability, facilitation, and depletion at central synapses. Neuron *18*, 995–1008.

Fee, M.S., Mitra, P.P., and Kleinfeld, D. (1996). Automatic sorting of multiple unit neuronal signals in the presence of anisotropic and non-Gaussian variability. J. Neurosci. Methods *69*, 175–188.

Fisher, S.A., Fischer, T.M., and Carew, T.J. (1997). Multiple overlapping processes underlying short-term synaptic enhancement. Trends Neurosci. *20*, 170–177.

Fortunato, C., Debanne, D., Scanziani, M., Gahwiler, B.H., and Thompson, S.M. (1996). Functional characterization and modulation of feedback inhibitory circuits in area CA3 of rat hippocampal slice cultures. Eur. J. Neurosci. *8*, 1758–1768.

Fox, S.E., and Ranck, J.B., Jr. (1981). Electrophysiological characteristics of hippocampal complex-spike cells and theta cells. Exp. Brain Res. *41*, 399–410.

Fox, S.E., Wolfson, S., and Ranck, J.B., Jr. (1986). Hippocampal theta rhythm and the firing of neurons in walking and urethane anesthetized rats. Exp. Brain Res. *62*, 495–508.

Freund, T.F., and Buzsáki, G. (1996). Interneurons of the hippocampus. Hippocampus *6*, 347–470.

Gallyas, F., Guldner, F.H., Zoltay, G., and Wolff, J.R. (1990). Golgi-like demonstration of "dark" neurons with an argyrophil III method for experimental neuropathology. Acta Neuropathol. (Berl.) *79*, 620–628.

Geiger, J.R., Lubke, J., Roth, A., Frotscher, M., and Jonas, P. (1997). Submillisecond AMPA receptor–mediated signaling at a principal neuron–interneuron synapse. Neuron *18*, 1009–1023.

Gray, C.M., Maldonado, P.E., Wilson, M., and McNaughton, B. (1995). Tetrodes markedly improve the reliability and yield of multiple single-unit isolation from multi-unit recordings in cat striate cortex. J. Neurosci. Methods *63*, 43–54.

Gulyas, A.I., Miles, R., Sik, A., Toth, K., Tamamaki, N., and Freund, T.F. (1993). Hippocampal pyramidal cells excite inhibitory neurons through a single release site. Nature *366*, 683–687.

Hessler, N.A., Shirke, A.M., and Malinow, R. (1993). The probability of transmitter release at a mammalian central synapse. Nature *366*, 569–572.

Jefferys, J.G., Traub, R.D., and Whittington, M.A. (1996). Neuronal networks for induced '40 Hz' rhythms. Trends Neurosci. *19*, 202–208.

Kubie, J.L., Muller, R.U., and Bostock, E. (1990). Spatial firing properties of hippocampal theta cells. J. Neurosci. *10*, 1110–1123.

Lacaille, J.-C., Mueller, A.L., Kunkel, D.D., and Schwartzkroin, P.A. (1987). Local circuit interactions between alveus/oriens interneurons and CA1 pyramidal cells in hippocampal slices: electrophysiology and morphology. J. Neurosci. *7*, 1979–1993.

Lisman, J.E. (1997). Bursts as a unit of neural information: making unreliable synapses reliable. Trends Neurosci. *20*, 38–43.

Malinow, R., Otmakhov, N., Blum, K.I., and Lisman, J. (1994). Visualizing hippocampal synaptic function by optical detection of $Ca2^{+}$ entry through the N-methyl-D-aspartate channel. Proc. Natl. Acad. Sci. USA *91*, 8170–8174.

Markram, H., Lubke, J., Frotscher, M., and Sakmann, B. (1997). Regulation of synaptic efficacy by coincidence of postsynaptic APs and EPSPs. Science *275*, 213–215.

McBain, C.J., and Maccaferri, G. (1997). Synaptic plasticity in hippocampal interneurons? A commentary. Can. J. Physiol. Pharmacol. *75*, 488–494.

McNaughton, B.L., Barnes, C.A., and O'Keefe, J. (1983). The contributions of position, direction, and velocity to single unit activity in the hippocampus of freely-moving rats. Exp. Brain Res. *52*, 41–49.

Miles, R. (1990). Synaptic excitation of inhibitory cells by single CA3 hippocampal pyramidal cells of the guinea-pig *in vitro*. J. Physiol. *428*, 61–77.

Miles, R., and Wong, R.K.S. (1986). Excitatory synaptic interactions between CA3 neurones in the guinea-pig hippocampus. J. Physiol. *373*, 397–418.

Nadasdy, Z., Csicsvari, J., Penttonen, M., Hetke, J., Wise, K., and Buzsáki, G. (1998). Extracellular recording and analysis of neuronal activity: from single cells to ensembles. In Large Scale Recording of Neuronal Activity, H. Eichenbaum and J. Davis, eds. (New York: J. Wiley and Sons), pp. 17–55.

O'Keefe, J., and Recce, M.L. (1993). Phase relationship between hippocampal place units and the EEG theta rhythm. Hippocampus *3*, 317–330.

Otmakhov, N., Shirke, A.M., and Malinow, R. (1993). Measuring the impact of probabilistic transmission on neuronal output. Neuron *10*, 1101–1111.

Perkel, D.H., Gerstein, G.L., and Moore, G.P. (1967). Neuronal spike trains and stochastic point processes. II. Simultaneous spiketrains. J. Neurophysiol. *7*, 419–440.

Perlman, G. (1980). Data analysis program for the UNIX operating system. Behav. Res. Methods Instrument. *12*, 554–558.

Press, W.H., Teukolsky, S.A., Vettering, W.T., and Flannery, B.P. (1992). Numerical Recipes in C: the Art of Scientific Computing, Second Edition (Cambridge: Cambridge University Press).

Raastad, M. (1995). Extracellular activation of unitary excitatory synapses between hippocampal CA3 and CA1 pyramidal cells. Eur. J. Neurosci. *7*, 1882–1888.

Rall, W. (1967). Distinguishing theoretical synaptic potentials computed for different soma-dendritic distributions of synaptic input. J. Neurophysiol. *30*, 1138–1168.

Ranck, J.B., Jr. (1973). Studies on single neurons in dorsal hippocampal formation and septum in unrestrained rats. I. Behavioral correlates and firing repertoires. Exp. Neurol. *41*, 461–531.

Reid, R.C., and Alonso, J.M. (1995). Specificity of monosynaptic connections from thalamus to visual cortex. Nature *378*, 281–284.

Shigemoto, R., Kulik, A., Roberts, J.D., Ohishi, H., Nusser, Z., Kaneko, T., and Somogyi, P. (1996). Target-cell–specific concentration of a metabotropic glutamate receptor in the presynaptic active zone. Nature *381*, 523–525.

Sik, A., Penttonen, M., Ylinen, A., and Buzsáki, G. (1995). Hippocampal CA1 interneurons: an *in vivo* intracellular labeling study. J. Neurosci. *15*, 6651–6665.

Skaggs, W.E., McNaughton, B.L., Wilson, M.A., and Barnes, C.A. (1996). Theta phase precession in hippocampal neuronal populations and the compression of temporal sequences. Hippocampus *6*, 149–172.

Stewart, M., and Fox, S.E. (1990). Do septal neurons pace the hippocampal theta rhythm? Trends Neurosci. *13*, 163–168.

Tanaka, K. (1983). Cross-correlation analysis of geniculostriate neuronal relationships in cats. J. Neurophysiol. *49*, 1303–1318.

Thompson, L.T., and Best, P.J. (1989). Place cells and silent cells in the hippocampus of freely-behaving rats. J. Neurosci. *9*, 2382–2390.

Thomson, A.M., and Deuchars, J. (1997). Synaptic interactions in neocortical local circuits: dual intracellular recordings *in vitro*. Cereb. Cortex *7*, 510–522.

Traub, R.D., and Miles, R. (1995). Pyramidal cell-to-inhibitory cell spike transduction explicable by active dendritic conductances in inhibitory cell. J. Comput. Neurosci. *2*, 291–298.

Tsodyks, M.V., and Markram, H. (1997). The neural code between neocortical pyramidal neurons depends on neurotransmitter release probability. Proc. Natl. Acad. Sci. USA *94*, 719–723.

Tsodyks, M.V., Skaggs, W.E., Sejnowski, T.J., and McNaughton, B.L. (1997). Paradoxical effects of external modulation of inhibitory interneurons. J. Neurosci. *17*, 4382–4388.

Wilson, M.A., and McNaughton, B.L. (1993). Dynamics of the hippocampal ensemble code for space. Science *261*, 1055–1058.

Ylinen, A., Bragin, A., Nadasdy, Z., Jando, G., Szabo, I., Sik, A., and Buzsáki, G. (1995). Sharp wave–associated high-frequency oscillation (200 Hz) in the intact hippocampus: network and intracellular mechanisms. J. Neurosci. *15*, 30–46.

Zador, A.M., and Dobrunz, L.E. (1997). Dynamic synapses in the cortex. Neuron *19*, 1–4.

Zucker, R.S. (1989). Short-term synaptic plasticity. Annu. Rev. Neurosci. *12*, 13–31.